

# Frequency-Dependent Vibronic Effects in Steady State Energy Transport

Leonardo F. Calderón\* and Paul Brumer\*

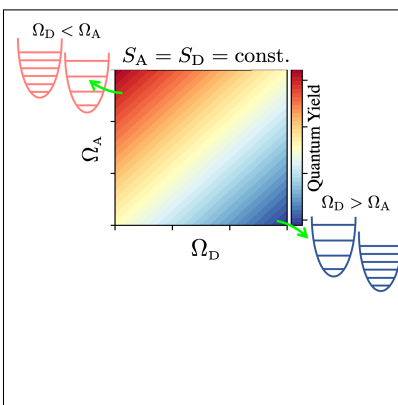
*Chemical Physics Theory Group, Department of Chemistry, and Center for Quantum  
Information and Quantum Control, University of Toronto, Toronto, Ontario M5S 3H6,  
Canada*

E-mail: [leonardo.calderon@utoronto.ca](mailto:leonardo.calderon@utoronto.ca); [paul.brumer@utoronto.ca](mailto:paul.brumer@utoronto.ca)

## Abstract

The interplay between electronic and intramolecular high-frequency vibrational degrees of freedom is ubiquitous in natural light-harvesting systems. Recent studies have indicated that an intramolecular vibrational donor-acceptor frequency difference can enhance energy transport. Here, we analyze the extent to which different intramolecular donor-acceptor vibrational frequencies affect excitation energy transport in equilibrium (coherent light excitation) and the more natural nonequilibrium steady state (incoherent light excitation) configurations. It is found that if the Huang-Rhys factors remain constant, the acceptor population increases when the intramolecular vibrational frequency of the acceptor exceeds that of the donor. The increase in the acceptor population due to the vibrational frequency difference is higher for higher values of the Huang-Rhys factors or the vibronic coupling strengths. However, the nonequilibrium steady state results show that the vibrational donor-acceptor frequency difference does not significantly enhance energy transport in the natural scenario of incoherent light excitation and under biologically relevant parameters. Insight about a potential mechanism to optimize energy transfer in the NESS based on increasing the harvesting time at the reaction center is analyzed.

## TOC Graphic



**Introduction.**—Excitation energy transport in natural light-harvesting systems (LHS), e.g., photosynthetic pigment-protein complexes, has been intensively studied with an aim of extracting design principles applicable to artificial (human-made) light-harvesting systems.<sup>1-4</sup> It is worth noting that the interaction between molecular electronic and vibrational degrees of freedom influences the energy transfer in LHS.<sup>3,5-26</sup> The vibrational degrees of freedom can be classified as inter- and intramolecular vibrational modes. The intermolecular vibrational modes are usually modeled as a low-frequency phonon bath characterized by a spectral density. The intramolecular vibrational modes are considered as discrete underdamped vibrations of high-frequency. Experimental spectra results of photosynthetic pigment-protein complexes indicate the presence of several intramolecular vibrational modes with different frequencies and strengths coupling to the electronic degrees of freedom.<sup>8,15,27-29</sup> Despite different high-energy vibrational frequency modes in the spectra, most theoretical models of light harvesting systems accounting for vibronic effects consider couplings to vibrational modes of the same frequency.

Recently, it has been reported that the energy transfer quantum yield in a prototype photosynthetic dimer is enhanced when the donor is coupled to a vibrational mode whose frequency is larger than that on the vibrational mode coupled to the acceptor.<sup>30</sup> In this donor-acceptor energy transfer,<sup>30</sup> it was assumed that the entire population is initially in the donor chromophore, representing a scenario commonly considered under coherent light excitation conditions. These laboratory-designed/controlled conditions contrast with those in nature, where the natural light-harvesting systems are continuously illuminated by incoherent radiation (sunlight),<sup>31-41</sup> leading to a nonequilibrium steady state (NESS).<sup>37,40-44</sup> In this Letter, we examine the conditions that lead to an increase in the quantum yield for both equilibrium and nonequilibrium steady states for coherent (laboratory) and incoherent (natural) light excitation, considering different intramolecular vibrational donor-acceptor frequencies and different Huang-Rhys factors for a prototypical photosynthetic dimer.

It is important to note that for energy transfer technologies even small improvements in

energy transfer, e.g. 5%, can be significant. Here we show that if such improvements are seen in equilibrium they are washed out in the NESS regime. Furthermore, in the particular case of biophysical systems we show that, contrary to some suggestions in the literature, donor-acceptor frequency differences do not significantly affect energy transfer.

We consider a prototype photosynthetic electronic dimer, adopting parameters typical of the Fenna-Matthews-Olson (FMO) complex.<sup>8,15,27-29</sup> The dimer is immersed in a protein-solvent environment modeled as a vibrational thermal bath at 300 K, composed of intra- and intermolecular vibrational modes and describe the incoherent light as a blackbody radiation thermal bath at 5600 K.<sup>36,45</sup> Additionally, exciton recombination and harvesting are considered. We solve for the equilibrium and nonequilibrium steady state using the numerically exact hierarchical equations of motion (HEOM) method.<sup>46-51</sup> The steady state acceptor population is regarded as the criterion to evaluate the energy transfer efficiency from donor to acceptor.

In this letter, we analyze the steady state acceptor population for different intramolecular vibrational donor-acceptor frequencies, Huang-Rhys factors, and vibronic coupling strengths in an equilibrium configuration (dimer + vibrational bath only), and in the nonequilibrium configuration (dimer + vibrational bath + radiation bath + exciton recombination and harvesting). In doing so, we demonstrate, for example, and as noted above, that in the natural scenario of incoherent light excitation and under biologically relevant parameters, the vibrational donor-acceptor frequency difference does not significantly enhance energy transport. In addition, we correct recently published erroneous results,<sup>30</sup> for the equilibrium steady state case, which states that the acceptor population increases when the intramolecular vibrational frequency of the donor is larger than at the acceptor for constant Huang-Rhys factors. Furthermore, we find that if the vibronic coupling strengths are fixed, the acceptor population will increase when the vibrational frequency of the donor is larger than at the acceptor.

*Model.*—Consider a prototype photosynthetic complex modeled as a dimer (donor-

acceptor (D-A) configuration) immersed within a protein-solvent environment. We assume an electronic dimer model representing the system of interest using open quantum system methodology and described through the Frenkel Hamiltonian

$$\hat{H}_{\text{Sys}} = \varepsilon_{\text{D}} \hat{\varphi}_{\text{D}}^+ \hat{\varphi}_{\text{D}}^- + \varepsilon_{\text{A}} \hat{\varphi}_{\text{A}}^+ \hat{\varphi}_{\text{A}}^- + V_{\text{DA}} (\hat{\varphi}_{\text{D}}^+ \hat{\varphi}_{\text{A}}^- + \hat{\varphi}_{\text{A}}^+ \hat{\varphi}_{\text{D}}^-). \quad (1)$$

The two first terms of the right-hand side of Eq. 1 account for the donor (acceptor) excited state electronic energies  $\varepsilon_{\text{D}}$  ( $\varepsilon_{\text{A}}$ ), and the last term for the excitonic coupling  $V_{\text{DA}}$ . The electronic excitation creation (annihilation) operators  $\hat{\varphi}_{\text{D,A}}^+$  ( $\hat{\varphi}_{\text{D,A}}^-$ ) are defined by  $|\varepsilon_{\text{D,A}}\rangle = \hat{\varphi}_{\text{D,A}}^+ |g_{\text{D,A}}\rangle$ ,  $|g_{\text{D,A}}\rangle = \hat{\varphi}_{\text{D,A}}^- |\varepsilon_{\text{D,A}}\rangle$ . We consider the two-level approximation on each site, where only the electronic ground state  $|g_{\text{D,A}}\rangle$  and the electronic first excited state  $|\varepsilon_{\text{D,A}}\rangle$  are taken into account. The eigenstates of system  $\hat{H}_{\text{Sys}} |e_i\rangle = E_{e_i} |e_i\rangle$  denote the exciton basis  $\{|e_+\rangle, |e_-\rangle\}$ , where the exciton states can be defined as linear superpositions of the electronic site states  $|e_i\rangle = \sum_j^{\text{D,A}} c_{ij} |\varepsilon_j\rangle$ , with energies  $E_{e_{\pm}} = \frac{\varepsilon_{\text{A}} + \varepsilon_{\text{D}}}{2} \pm \frac{1}{2} \sqrt{\Delta\varepsilon^2 + 4V_{\text{DA}}^2}$ , and where  $\Delta\varepsilon = \varepsilon_{\text{D}} - \varepsilon_{\text{A}}$  is the site energy difference.

The protein-solvent environment is considered as a collection of harmonic vibrational modes. This vibrational bath is composed of both intra- and intermolecular vibrational modes. The Hamiltonian for the vibrational bath reads

$$\hat{H}_{\text{VB}} = \hbar\Omega_{\text{D}} \hat{\mathbf{b}}_{\text{D}}^\dagger \hat{\mathbf{b}}_{\text{D}} + \hbar\Omega_{\text{A}} \hat{\mathbf{b}}_{\text{A}}^\dagger \hat{\mathbf{b}}_{\text{A}} + \sum_i^{\text{D,A}} \sum_j \hbar\omega_j^{(i)} \hat{b}_j^{(i)\dagger} \hat{b}_j^{(i)}. \quad (2)$$

We consider only one intramolecular vibrational on each site. The creation (annihilation) operators for the intramolecular vibrational modes of frequencies  $\Omega_{\text{D}}$  and  $\Omega_{\text{A}}$  are denoted by the calligraphic letters  $\hat{\mathbf{b}}_{\text{D,A}}^\dagger$ , ( $\hat{\mathbf{b}}_{\text{D,A}}$ ). The creation (annihilation) operators for the intermolecular vibrational modes of frequencies  $\omega_l^{(i)}$  are denoted by  $\hat{b}_l^{(i)\dagger}$ , ( $\hat{b}_l^{(i)}$ ).

The interaction between the system and the vibrational bath is given by the Hamiltonian

$$\begin{aligned} \hat{H}_{\text{Sys-VB}} = & \hbar\mathcal{G}_{\text{D}}\hat{\varphi}_{\text{D}}^+\hat{\varphi}_{\text{D}}^- \left( \hat{\mathbf{b}}_{\text{D}}^\dagger + \hat{\mathbf{b}}_{\text{D}} \right) + \hbar\mathcal{G}_{\text{A}}\hat{\varphi}_{\text{A}}^+\hat{\varphi}_{\text{A}}^- \left( \hat{\mathbf{b}}_{\text{A}}^\dagger + \hat{\mathbf{b}}_{\text{A}} \right) \\ & + \sum_i^{\text{D,A}} \sum_j \hbar g_j^{(i)} \hat{\varphi}_i^+ \hat{\varphi}_i^- \left( \hat{b}_j^{(i)} + \hat{b}_j^{(i)\dagger} \right), \end{aligned} \quad (3)$$

where  $\mathcal{G}_{\text{D}} = \sqrt{S_{\text{D}}}\Omega_{\text{D}}$  ( $\mathcal{G}_{\text{A}} = \sqrt{S_{\text{A}}}\Omega_{\text{A}}$ ) denotes the coupling between the electronic donor (acceptor) state and the intramolecular vibrational mode of frequency  $\Omega_{\text{D}}$  ( $\Omega_{\text{A}}$ ) (referred to below as vibronic coupling), where  $S_{\text{D}}$  ( $S_{\text{A}}$ ) is the dimensionless Huang-Rhys factor at the donor (acceptor). In Eq. 3,  $g_j^{(\text{D})}$  ( $g_j^{(\text{A})}$ ) represents the coupling between the electronic donor (acceptor) state and the  $j^{\text{th}}$  intermolecular vibrational mode. Therefore, the global Hamiltonian for the prototype photosynthetic complex is given by  $\hat{H} = \hat{H}_{\text{Sys}} + \hat{H}_{\text{Sys-VB}} + \hat{H}_{\text{VB}}$ .

All the information about the vibrational bath is encoded in the spectral density of the donor and acceptor

$$\begin{aligned} J_{\text{D,A}}(\omega) = & J_{\text{intra}}(\omega) + J_{\text{inter}}(\omega) \\ = & \frac{4\Lambda_{\text{D,A}}\Gamma\Omega_{\text{D,A}}^2\omega}{(\Omega_{\text{D,A}}^2 - \omega^2)^2 + 4\Gamma^2\omega^2} + \frac{2\lambda\gamma\omega}{\hbar(\omega^2 + \gamma^2)}. \end{aligned} \quad (4)$$

The first term in Eq. 4 corresponds to the contribution of the intramolecular vibrational mode through an underdamped Brownian oscillator spectral density. The second term accounts for the intermolecular vibrational modes, corresponding to a low-frequency vibrational bath described by a Drude-Lorentz spectral density. Here,  $\Lambda_{\text{D,A}} = S_{\text{D,A}}\Omega_{\text{D,A}} = \sqrt{S_{\text{D,A}}}\mathcal{G}_{\text{D,A}}$  is the reorganization energy and  $\Gamma$  is the peak width (cut-off frequency). We assume independent baths on each site at temperature  $T^{\text{VB}} = 300$  K.

**Equilibrium steady state configuration.**—We analyze the effect of the vibrational bath described by Eqs. 2–4 on the energy transfer from the donor to the acceptor by examining acceptor population changes due to vibronic effects in the steady state. The entire population is initially assumed to be in the donor chromophore  $\rho_{\text{DD}}(t=0) = 1$ . This condi-

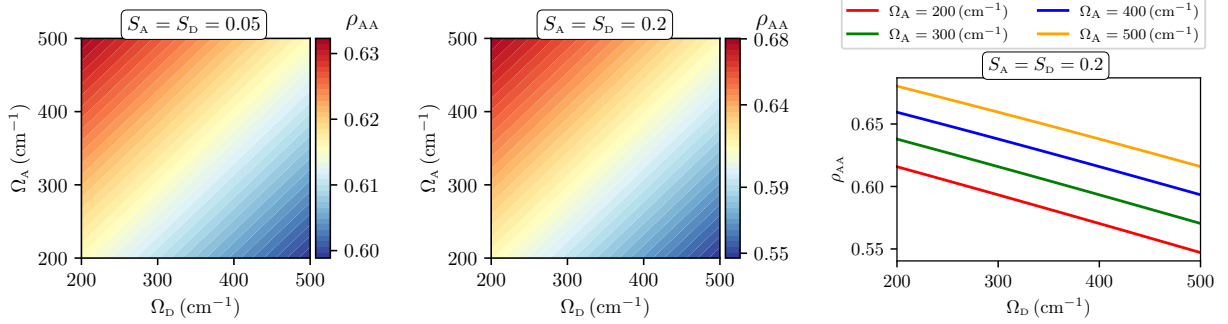


Figure 1: Equilibrium steady state acceptor population  $\rho_{AA}$  as a function of the intramolecular vibrational frequencies at the donor  $\Omega_D$  and the acceptor  $\Omega_A$  considering different fixed Huang-Rhys factors  $S_A = S_D = \{0.05, 0.2\}$ . The vibrational bath parameters are  $\lambda = 50 \text{ cm}^{-1}$ ,  $\gamma = 200 \text{ cm}^{-1}$ ,  $\Gamma = 10 \text{ cm}^{-1}$ , and  $T^{\text{VB}} = 300 \text{ K}$ .

tion is commonly considered under coherent light excitation conditions. Consistent with the literature in this scenario, the steady state corresponds to a thermal equilibrium state, where the acceptor population  $\rho_{AA}$  quantifies the quantum yield. Specifically, we consider different intramolecular vibrational donor and acceptor frequencies for several fixed Huang-Rhys factors and vibronic coupling strengths. Other physical effects, such as incoherent light excitation, exciton recombination and harvesting, are analyzed below. We assume parameters characteristic of prototypical photosynthetic complexes, such as the Fenna-Matthews-Olson (FMO) complex, i.e.,  $\Delta\varepsilon = 100 \text{ cm}^{-1}$ , with  $\varepsilon_D > \varepsilon_A$ ,  $V_{DA} = 50 \text{ cm}^{-1}$ , the excitonic energy splitting is given by  $\Delta E_e = 141.4 \text{ cm}^{-1}$ , and for the vibrational bath  $\lambda = 50 \text{ cm}^{-1}$ ,  $\gamma = 200 \text{ cm}^{-1}$ ,  $\Gamma = 10 \text{ cm}^{-1}$ , and  $T^{\text{VB}} = 300 \text{ K}$ .

Figure 1 depicts the thermal equilibrium acceptor population  $\rho_{AA}$  (quantum yield) as a function of the intramolecular vibrational donor  $\Omega_D$  and acceptor  $\Omega_A$  frequencies for two constant Huang-Rhys factors  $S_A = S_D = \{0.05, 0.2\}$ . The intramolecular vibrational frequencies satisfy  $\Omega_D, \Omega_A > \Delta\varepsilon, \Delta E_e, V_{DA}$ . Figure 1 shows that  $\rho_{AA}$  increases when the intramolecular vibrational frequency at the acceptor is larger than at the donor  $\Omega_A > \Omega_D$  and decreases when  $\Omega_A < \Omega_D$ . For constant Huang-Rhys factors  $S_A = S_D$ , the thermal equilibrium acceptor population decreases linearly\* with  $\Omega_D$  when  $\Omega_A$  is constant, i.e.,  $\rho_{AA}(\Omega_D; \Omega_A, S_A = S_D) \propto -\Omega_D$

\*The decrease in  $\rho_{AA}$  is no longer linear for large values of the Huang-Rhys factors ( $S_A = S_D \geq 1$ ).

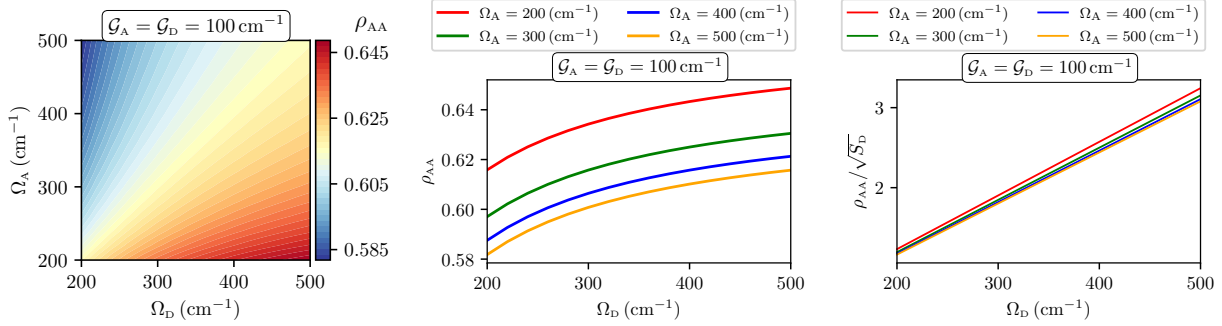


Figure 2: Equilibrium steady state acceptor population  $\rho_{AA}$  as a function of the intramolecular vibrational frequencies at the donor  $\Omega_D$  and the acceptor  $\Omega_A$  considering fixed vibronic coupling strengths  $\mathcal{G}_A = \mathcal{G}_D = 100 \text{ cm}^{-1}$ . The vibrational bath parameters are  $\lambda = 50 \text{ cm}^{-1}$ ,  $\gamma = 200 \text{ cm}^{-1}$ ,  $\Gamma = 10 \text{ cm}^{-1}$ , and  $T^{\text{VB}} = 300 \text{ K}$ .

(see the right panel in Figure 1). In this case,  $\rho_{AA}$  becomes larger when  $\Omega_A > \Omega_D$  because the vibronic coupling in the acceptor is larger than in the donor, i.e.,  $G_A > G_D$ . That means, for instance, when  $\Omega_A$  is constant ( $G_A$  is also constant), if  $\Omega_D$  increases, then  $G_D$  increases, since  $S_D$  is constant, which leads to lower eigenenergies at the donor and, therefore larger donor populations and lower acceptor populations (thermal equilibrium distribution).

Figure 1 shows that when  $S_A$  and  $S_D$  increase, the maximum and minimum of  $\rho_{AA}$  increases and decreases, respectively. The latter is a consequence of the increase in the vibronic coupling, which leads to lower and higher eigenenergies. For relevant biological values of the Huang-Rhys factors:  $S_A = S_D = 0.05$ ,  $\rho_{AA}$  changes by up to  $\sim 5\%$ . Hence, devices designed for enhanced energy transfer would benefit from larger Huang-Rhys factors. The changes in  $\rho_{AA}$  are marginal when  $\Omega_A = \Omega_D$  ( $\lesssim 0.1\%$ ), i.e., values along the diagonal. Note that the results for  $S_A = S_D = 0.2$  (middle panel in Figure 1) were recently obtained incorrectly,<sup>30</sup> being opposite to the results presented in this Letter.

Figure 2 shows the thermal equilibrium acceptor population  $\rho_{AA}$  (quantum yield) as a function of  $\Omega_D$  and  $\Omega_A$  for a constant vibronic coupling strength  $G_A = G_D = 100 \text{ cm}^{-1}$ . Figure 2 shows that  $\rho_{AA}$  increases when the intramolecular vibrational frequency at the donor is larger than at the acceptor  $\Omega_A < \Omega_D$  and decreases when  $\Omega_A > \Omega_D$  ( $\rho_{AA}$  changes by up to  $\sim 11\%$ ). This contrasts with the case of constant Huang-Rhys factors discussed



above. For constant vibronic coupling strengths  $\mathcal{G}_A = \mathcal{G}_D$ , the thermal equilibrium acceptor population increases proportionally to  $\sqrt{S_D} \Omega_D$  when  $\Omega_A$  is constant, i.e.,  $\rho_{AA}(\Omega_D; \Omega_A, \mathcal{G}_A = \mathcal{G}_D) \propto \sqrt{S_D} \Omega_D$  (see the middle panel in Figure 2). To confirm this, the right panel of Figure 2 shows that  $\rho_{AA}/\sqrt{S_D}$  grows linearly<sup>†</sup> with  $\Omega_D$  when  $\Omega_A$  is constant. That means, for instance, when  $\Omega_A$  is constant, if  $\Omega_D$  increases, then the donor eigenenergies will be higher, since  $\mathcal{G}_D$  is constant, which leads to lower donor populations and larger acceptor populations (thermal equilibrium distribution). Note that  $S_D$  varies inversely with  $\Omega_D$ , in contrast to the constant Huang-Rhys factors  $S_A = S_D$  analyzed above. Hence, for constant vibronic coupling strengths  $\mathcal{G}_A = \mathcal{G}_D$ ,  $\rho_{AA}$  becomes larger when  $\Omega_A < \Omega_D$  ( $S_A > S_D$ ).

We recently examined the role of the electronic-vibrational (vibronic) resonance in the nonequilibrium steady state transport of the PEB dimer in the cryptophyte algae PE545.<sup>41</sup> We found that an equilibrium steady state reached due to the interaction with a thermal bath is not sensitive to vibronic resonance. This is also confirmed for the dimer analyzed here. When the intramolecular vibrational frequencies at the donor and acceptor are in resonance with the excitonic energy splitting  $\Omega_D, \Omega_A \approx \Delta E_e$  (i.e.,  $\Omega_D = \Omega_A = 142 \text{ cm}^{-1}$ ), the changes in the thermal equilibrium acceptor population  $\rho_{AA}$  compared to off-resonance frequencies are insignificant ( $\lesssim 0.05\%$ ). The analysis and conclusions obtained so far remain valid when  $\varepsilon_D < \varepsilon_A$  with the same parameters considered before.

***Nonequilibrium steady state configuration.***—The scenario analyzed above, i.e., a thermal equilibrium state reached when the system interacts with a vibration bath only, is often examined in the context of pulsed laser excitation, in which it is assumed, for example, that the coherent light source prepares an initial state in the molecular system with the entire population in the donor or the highest energy exciton state. The system then interacts with the vibrational bath and the energy transfer dynamics to the acceptor are analyzed.<sup>30</sup> However, this differs from natural conditions, in which the light-harvesting system is continuously illuminated with incoherent natural light,<sup>31–40</sup> such as sunlight and

---

<sup>†</sup>The increase in  $\rho_{AA}/\sqrt{S_D}$  is no longer linear for large values of the Huang-Rhys factors ( $S_A = S_D \geq 1$ ).

additional processes contribute. Here, we examine the effect of different intramolecular vibrational frequencies at the donor and acceptor in the nonequilibrium steady state energy transport under the influence of a vibrational bath (Eqs. 2–4), incoherent light excitation, exciton recombination, and exciton harvesting at the reaction center. We show below that any parameter dependencies observed in the equilibrium case for the acceptor population are washed out in the resultant NESS.

The interaction between the system and the radiation bath (incoherent light) is given by the Hamiltonian

$$\hat{H}_{\text{Sys-RB}} = -\hat{\boldsymbol{\mu}}_{\text{D}} \cdot \hat{\mathbf{E}}(t), \quad (5)$$

where  $\hat{\boldsymbol{\mu}}_{\text{D}}$  is the transition dipole operator of the donor, and  $\hat{\mathbf{E}}(t) = \hat{\mathbf{E}}^{(+)}(t) + \hat{\mathbf{E}}^{(-)}(t)$  is electric field,<sup>52</sup> with  $\hat{\mathbf{E}}^{(+)}(t) = i \sum_{\mathbf{k},s} \sqrt{\frac{\hbar\omega}{2\epsilon_0 V}} \hat{a}_{\mathbf{k},s} \mathbf{e}_{\mathbf{k},s} e^{-i\omega t}$  and  $\hat{\mathbf{E}}^{(-)}(t) = [\hat{\mathbf{E}}^{(+)}(t)]^\dagger$ . The creation (annihilation) operator for the  $\mathbf{k}^{\text{th}}$  radiation field mode in the  $s^{\text{th}}$  polarization state is denoted  $\hat{a}_{\mathbf{k},s}^\dagger$  ( $\hat{a}_{\mathbf{k},s}$ ), and  $\mathbf{e}_{\mathbf{k},s}$  is the radiation polarization vector. We assume that the transition electric dipole operator of the acceptor is perpendicular to the radiation polarization vector, i.e., only the donor chromophore is pumped by incoherent light. The latter is a typical scenario analyzed in the context of energy transfer.<sup>41,44,53</sup> The Hamiltonian for the radiation bath reads

$$\hat{H}_{\text{RB}} = \sum_{\mathbf{k},s} \hbar c k \hat{a}_{\mathbf{k},s}^\dagger \hat{a}_{\mathbf{k},s}. \quad (6)$$

The radiation bath is described by a super-Ohmic spectral density with cubic-frequency dependence

$$J_{\text{D}}^{\text{RB}}(\omega) = \frac{2\hbar\omega^3}{3(4\epsilon_0\pi^2c^3)}. \quad (7)$$

This spectral density generates long-lasting coherent dynamics provided by the lack of pure dephasing dynamics and by the strong dependence of the decoherence rate on the system level spacing.<sup>36</sup> The temperature assumed for the radiation bath is  $T^{\text{RB}} = 5600$  K, and the transition dipole moment is  $\mu_{\text{D}} = 6$  D.

We consider the exciton recombination accounting for the nonradiative electronic ex-

citation decay to the ground state as a localized process on each site and occurring on a nanosecond time scale (recombination time  $\tau_{\text{rec}}$ ).<sup>42-44,53,54</sup> The exciton recombination is described by the effective Lindbladian

$$\mathcal{L}_{\text{rec}}[\hat{\rho}] = \tau_{\text{rec}}^{-1} \sum_i^{\text{D,A}} \left( |g_i\rangle\langle\varepsilon_i|\hat{\rho}|\varepsilon_i\rangle\langle g_i| - \frac{1}{2} [|\varepsilon_i\rangle\langle\varepsilon_i|, \hat{\rho}]_+ \right), \quad (8)$$

where  $[\hat{\mathcal{O}}_1, \hat{\mathcal{O}}_2]_+$  denotes the anticommutator between operators  $\hat{\mathcal{O}}_1$  and  $\hat{\mathcal{O}}_2$ . The same recombination time for the donor and acceptor is taken as  $\tau_{\text{rec}} = 1$  ns.

The electronic excitation harvesting (trapping) at the reaction center occurs on a picosecond time scale (trapping time  $\tau_{\text{trap}}$ ). Under localized trapping conditions, only the acceptor chromophore is coupled to the reaction center, and the trapping process is modeled by the Lindbladian<sup>42-44,53,54</sup>

$$\mathcal{L}_{\text{trap}}^{(\text{loc})}[\hat{\rho}] = \tau_{\text{trap}}^{-1} \left( |\text{RC}\rangle\langle\varepsilon_{\text{A}}|\hat{\rho}|\varepsilon_{\text{A}}\rangle\langle\text{RC}| - \frac{1}{2} [|\varepsilon_{\text{A}}\rangle\langle\varepsilon_{\text{A}}|, \hat{\rho}]_+ \right). \quad (9)$$

For localized trapping conditions and under weak incoherent light excitation the NESS quantum yield  $\eta = \frac{\Gamma_{\text{RC}}}{r_{\text{abs}}}\rho_{\text{AA}}^{(\text{neq})}$  is proportional to the acceptor population  $\rho_{\text{AA}}^{(\text{neq})}$ , since the ground state population  $\rho_{gg} \simeq 1$  at all times.<sup>42,44</sup> Here  $\Gamma_{\text{RC}} = \tau_{\text{rec}}^{-1}/2$  is the trapping rate constant that quantifies the coupling strength to the reaction center, and  $r_{\text{abs}}$  is the incoherent light absorption rate.

Figure 3 shows the nonequilibrium steady state acceptor population  $\rho_{\text{AA}}^{(\text{neq})}$  as a function of the intramolecular vibrational donor  $\Omega_{\text{D}}$  and acceptor  $\Omega_{\text{A}}$  frequencies for different Huang-Rhys factors  $S_{\text{A}} = S_{\text{D}} = \{0.05, 0.2, 0.5\}$ , assuming localized trapping conditions. The values reported in color are  $10^{-5}$  smaller than those in Figure 1, reflecting the weak incident incoherent light, exciton harvesting and recombination effects.<sup>36,39,41</sup> We assume a recombination time  $\tau_{\text{rec}} = 1$  ns and a trapping time  $\tau_{\text{trap}} = 10$  ps. The displayed intramolecular vibrational frequencies satisfy  $\Omega_{\text{D}}, \Omega_{\text{A}} > \Delta\varepsilon, \Delta E_e, V_{\text{DA}}$ . Figure 3 shows that  $\rho_{\text{AA}}^{(\text{neq})}$  increases when the intramolecular vibrational frequency at the acceptor is larger than at the donor  $\Omega_{\text{A}} > \Omega_{\text{D}}$ .

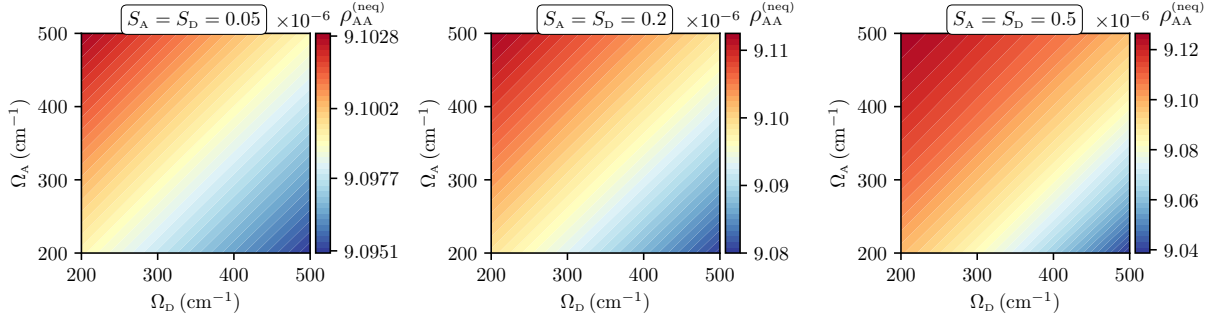


Figure 3: Nonequilibrium steady state acceptor population  $\rho_{AA}^{(\text{neq})}$  as a function of the intramolecular vibrational frequencies at the donor  $\Omega_D$  and the acceptor  $\Omega_A$  considering different fixed Huang-Rhys factors  $S_A = S_D = \{0.05, 0.2, 0.5\}$  for localized trapping conditions. The baths parameters are  $\lambda = 50 \text{ cm}^{-1}$ ,  $\gamma = 200 \text{ cm}^{-1}$ ,  $\Gamma = 10 \text{ cm}^{-1}$ ,  $T^{\text{VB}} = 300 \text{ K}$ ,  $T^{\text{RB}} = 5600 \text{ K}$ . Typical values for recombination  $\tau_{\text{rec}} = 1 \text{ ns}$  and trapping  $\tau_{\text{trap}} = 10 \text{ ps}$  times are assumed. Note that the color scales are on the order of  $10^{-6}$ .

Therefore, when  $\Omega_A$  is constant,  $\rho_{AA}^{(\text{neq})}$  decreases when  $\Omega_D$  increases. Figure 3 shows that as  $S_A$  and  $S_D$  increase, the maximum and minimum of  $\rho_{AA}^{(\text{neq})}$  increase and decrease, respectively. The color pattern displayed in Figure 3 is similar to that of the top panels in Figure 1, for the thermal equilibrium state. However, the changes in  $\rho_{AA}^{(\text{neq})}$  are seen to be insignificant ( $< 1\%$ ) for all Huang-Rhys factors considered. When the trapping time  $\tau_{\text{trap}}$  increases by one order of magnitude, e.g.,  $\tau_{\text{trap}} = 100 \text{ ps}$ ,  $\rho_{AA}^{(\text{neq})}$  also increases by one order of magnitude, and the changes the  $\rho_{AA}^{(\text{neq})}$  are  $\sim 3\%$  ( $S = 0.2$ ) (data not shown). Therefore, increasing the trapping time would enhance the energy transfer in the NESS.

In the nonequilibrium steady state, the population flux between the donor and acceptor is linked to the imaginary part of the intersite coherence.<sup>41,44,55–57</sup> Here, we find that the nonequilibrium steady state intersite coherence displays the same trend as for  $\rho_{AA}^{(\text{neq})}$  in Figure 3 (Figure not shown). In addition, the case of constant vibronic coupling strengths  $\mathcal{G}_A = \mathcal{G}_D = 100 \text{ cm}^{-1}$  was also considered with similar results. The pattern of change in the nonequilibrium steady state acceptor population  $\rho_{AA}^{(\text{neq})}$  is similar to that presented for the equilibrium steady state above, and the changes  $\rho_{AA}^{(\text{neq})}$  as those discussed in Figure 3. Furthermore, even if the reorganization energy increases to  $\lambda = 100 \text{ cm}^{-1}$ , i.e., twice the value previously considered, and still within the relevant range expected under biological

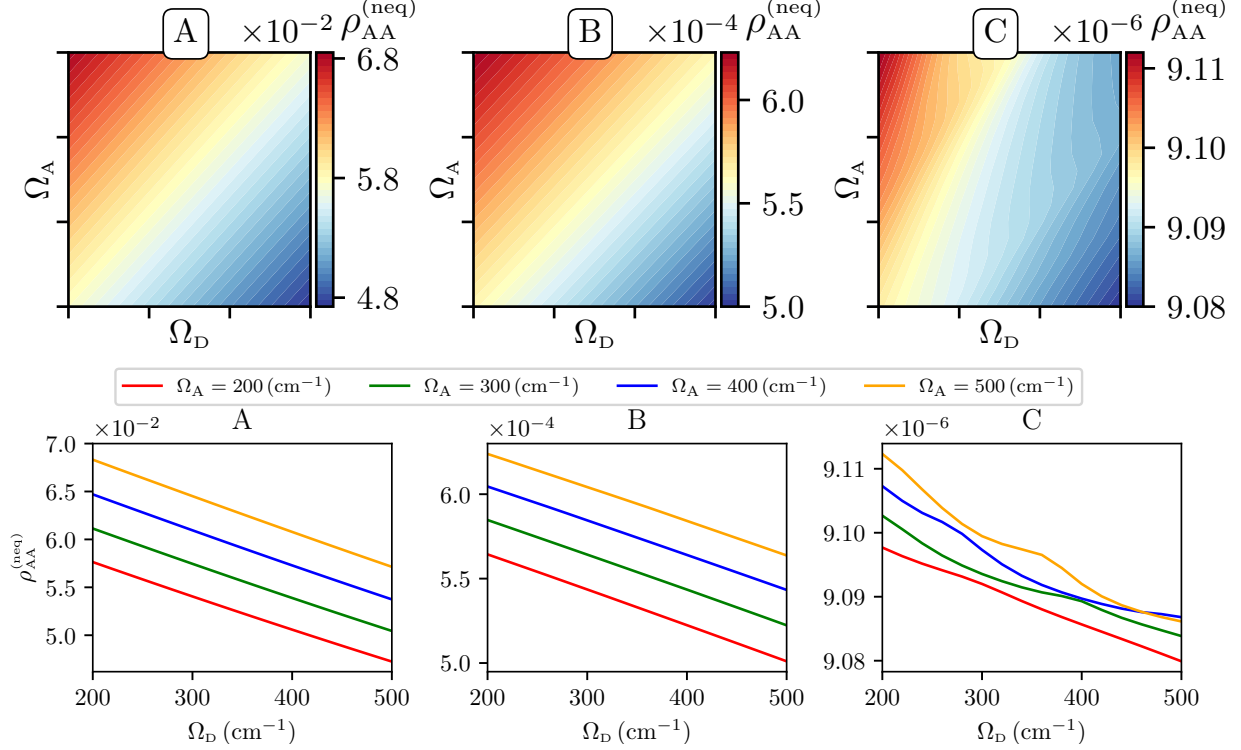


Figure 4: Nonequilibrium steady state acceptor population  $\rho_{AA}^{(\text{neq})}$  as a function of the intramolecular vibrational frequency at the donor  $\Omega_D$  and acceptor frequencies  $\Omega_A$ . We consider different scenarios for the NESS, radiation and vibrational baths only (panel A), radiation bath and exciton recombination only (panel B), radiation bath, and exciton recombination and localized exciton trapping (panel C). We assume the Huang-Rhys factors  $S = S_A = S_D = 0.2$ . The vibrational bath parameters are  $\lambda = 50 \text{ cm}^{-1}$ ,  $\gamma = 200 \text{ cm}^{-1}$ ,  $\Gamma = 10 \text{ cm}^{-1}$ , and  $T^{\text{VB}} = 300 \text{ K}$ . Typical values for recombination  $\tau_{\text{rec}} = 1 \text{ ns}$  and trapping  $\tau_{\text{trap}} = 10 \text{ ps}$  times are assumed. Note the differences in the vertical scale.

conditions, changes in the acceptor population are still insignificant (Figure not shown).

Even though the natural scenario approximates the picture discussed above, where the exciton population is collected at the reaction center and excitons have a finite lifetime (exciton recombination), we examine individual non-unitary contributions to evaluate the effect of the donor-acceptor intramolecular vibrational frequency difference in the NESS acceptor population. Figure 4 depicts the acceptor population  $\rho_{AA}^{(\text{neq})}$  as a function of  $\Omega_D$  and  $\Omega_A$  for a fixed Huang-Rhys factor  $S_A = S_D = 0.2$ , considering that the system only interacts with: the incoherent light and the vibrational bath (panel A), the incoherent light and also undergoes exciton recombination (panel B), and the incoherent light and also undergoes

exciton recombination and localized trapping (panel C). In all the cases,  $\rho_{AA}^{(\text{neq})}$  is larger when  $\Omega_A > \Omega_D$  and decreases as  $\Omega_D$  increases. Figure 4 shows that  $\rho_{AA}^{(\text{neq})}$  decreases linearly with  $\Omega_D$  for panels A and B (no exciton harvesting), but when the effect of exciton trapping is included, the decrease is no longer linear. Therefore, the nonlinear variation of  $\rho_{AA}^{(\text{neq})}$  with  $\Omega_D$  is caused by exciton trapping at the reaction center, and increases when the trapping time  $\tau_{\text{trap}}$  decreases. In addition, as discussed above for the equilibrium case, the nonlinearity also increases when the Huang-Rhys factors increase. It is important to note that when the system interacts with the incoherent light and the vibrational bath only, the NESS reached allows for significant changes up to 40% in  $\rho_{AA}^{(\text{neq})}$  (panel A). Under this scenario the interaction with the vibrational bath is stronger than the interaction with incoherent light. Therefore, it is the exciton harvesting at the reaction center that washes out the variations in the acceptor population related to the donor-acceptor intramolecular vibrational frequency difference displayed in the thermal equilibrium case.

In conclusion, the HEOM method was used to analyze the effect of different intramolecular vibrational frequencies on energy transfer in a prototype photosynthetic dimer system, under both equilibrium (ESS) and nonequilibrium steady state (NESS) conditions. When an equilibrium thermal state is reached by the interaction of the system only with a vibrational bath, the results indicate that, for constant Huang-Rhys factors, the thermal equilibrium acceptor population (quantum yield) decreases with an increasing vibrational donor frequency for a constant vibrational acceptor frequency. That is, the acceptor population increases when the vibrational frequency of the acceptor is larger than in the donor because the vibronic coupling in the acceptor is larger than in the donor. Conversely, for constant vibronic coupling strengths, the acceptor population increases proportionally to the square root of the donor Huang-Rhys factor times the vibrational donor frequency for a constant vibrational acceptor frequency. In this case, the quantum yield increases when the vibrational frequency of the donor is larger than in the acceptor because the Huang-Rhys factor in the acceptor is larger than in the donor.

In the NESS, and considering constant Huang-Rhys factors, the variations in the acceptor population for localized trapping conditions are much smaller than those of the thermal equilibrium quantum yield. Therefore, under natural biological conditions of incoherent light excitation, the NESS reached does not allow for a significant enhancement in the quantum yield due to the intramolecular vibrational frequency difference. Technologically, however, one can increase the quantum yield somewhat by increasing the trapping time. For example, increasing the trapping time by one order of magnitude increases the acceptor population by one order of magnitude, with a higher variation with the donor-acceptor intramolecular vibrational frequency difference. Therefore, increasing the trapping time is a possible mechanism to enhance the energy transfer in the NESS. In the future, it would be interesting to examine more realistic exciton trapping scenarios beyond the effective Lindblad methodology considered in this Letter.

## Acknowledgement

This work was supported by the U.S. Air Force Office of Scientific Research (AFOSR) under Contract No. FA9550-20-1-0354.

## References

- (1) Scholes, G. D.; Fleming, G. R.; Olaya-Castro, A.; van Grondelle, R. Lessons From Nature About Solar Light Harvesting. *Nat. Chem.* **2011**, *3*, 763–774.
- (2) Romero, E.; Novoderezhkin, V. I.; van Grondelle, R. Quantum Design of Photosynthesis for Bio-Inspired Solar-Energy Conversion. *Nature* **2017**, *543*, 355–365.
- (3) Cao, J.; Cogdell, R. J.; Coker, D. F.; Duan, H.-G.; Hauer, J.; Kleinekathöfer, U.; Jansen, T. L.; Mančal, T.; Miller, R. D.; Ogilvie, J. P. et al. Quantum Biology Revisited. *Sci. Adv.* **2020**, *6*, eaaz4888.

- (4) Mančal, T. A Decade With Quantum Coherence: How Our Past Became Classical and the Future Turned Quantum. *Chem. Phys.* **2020**, *532*, 110663.
- (5) Prior, J.; Chin, A. W.; Huelga, S. F.; Plenio, M. B. Efficient Simulation of Strong System-Environment Interactions. *Phys. Rev. Lett.* **2010**, *105*, 050404.
- (6) Womick, J. M.; Moran, A. M. Vibronic Enhancement of Exciton Sizes and Energy Transport in Photosynthetic Complexes. *J. Phys. Chem. B* **2011**, *115*, 1347–1356.
- (7) Butkus, V.; Valkunas, L.; Abramavicius, D. Molecular Vibrations-Induced Quantum Beats in Two-Dimensional Electronic Spectroscopy. *J. Chem. Phys.* **2012**, *137*, 044513.
- (8) Christensson, N.; Kauffmann, H. F.; Pullerits, T. o.; Mančal, T. Origin of Long-Lived Coherences in Light-Harvesting Complexes. *J. Phys. Chem. B* **2012**, *116*, 7449–7454.
- (9) Kolli, A.; O'Reilly, E. J.; Scholes, G. D.; Olaya-Castro, A. The Fundamental Role of Quantized Vibrations in Coherent Light Harvesting by Cryptophyte Algae. *J. Chem. Phys.* **2012**, *137*, 174109.
- (10) Chenu, A.; Christensson, N.; Kauffmann, H. F.; Mančal, T. Enhancement of Vibronic and Ground-State Vibrational Coherences in 2D Spectra of Photosynthetic Complexes. *Sci. Rep.* **2013**, *3*, 2029.
- (11) Tiwari, V.; Peters, W. K.; Jonas, D. M. Electronic Resonance With Anticorrelated Pigment Vibrations Drives Photosynthetic Energy Transfer Outside the Adiabatic Framework. *Proc. Natl. Acad. Sci. U.S.A.* **2013**, *110*, 1203–1208.
- (12) Chin, A. W.; Prior, J.; Rosenbach, R.; Caycedo-Soler, F.; Huelga, S. F.; Plenio, M. B. The Role of Non-Equilibrium Vibrational Structures in Electronic Coherence and Re-coherence in Pigment-Protein Complexes. *Nat. Phys.* **2013**, *9*, 113–118.
- (13) Fuller, F. D.; Pan, J.; Gelzinis, A.; Butkus, V.; Senlik, S. S.; Wilcox, D. E.;



- Yocum, C. F.; Valkunas, L.; Abramavicius, D.; Ogilvie, J. P. Vibronic Coherence in Oxygenic Photosynthesis. *Nat. Chem.* **2014**, *6*, 706–711.
- (14) Butkus, V.; Valkunas, L.; Abramavicius, D. Vibronic Phenomena and Exciton-Vibrational Interference in Two-Dimensional Spectra of Molecular Aggregates. *J. Chem. Phys.* **2014**, *140*, 034306.
- (15) Halpin, A.; Johnson, P. J.; Tempelaar, R.; Murphy, R. S.; Knoester, J.; Jansen, T. L.; Miller, R. D. Two-Dimensional Spectroscopy of a Molecular Dimer Unveils the Effects of Vibronic Coupling on Exciton Coherences. *Nat. Chem.* **2014**, *6*, 196–201.
- (16) O'Reilly, E. J.; Olaya-Castro, A. Non-Classicality of the Molecular Vibrations Assisting Exciton Energy Transfer at Room Temperature. *Nat. Commun.* **2014**, *5*, 3012.
- (17) Romero, E.; Augulis, R.; Novoderezhkin, V. I.; Ferretti, M.; Thieme, J.; Zigmantas, D.; Van Grondelle, R. Quantum Coherence in Photosynthesis for Efficient Solar Energy Conversion. *Nat. Phys.* **2014**, *10*, 676–682.
- (18) Dijkstra, A. G.; Wang, C.; Cao, J.; Fleming, G. R. Coherent Exciton Dynamics in the Presence of Underdamped Vibrations. *J. Phys. Chem. Lett.* **2015**, *6*, 627–632.
- (19) Novelli, F.; Nazir, A.; Richards, G. H.; Roozbeh, A.; Wilk, K. E.; Curmi, P. M.; Davis, J. A. Vibronic Resonances Facilitate Excited-State Coherence in Light-Harvesting Proteins at Room Temperature. *J. Phys. Chem. Lett.* **2015**, *6*, 4573–4580.
- (20) Schröter, M.; Ivanov, S.; Schulze, J.; Polyutov, S.; Yan, Y.; Pullerits, T.; Kühn, O. Exciton–Vibrational Coupling in the Dynamics and Spectroscopy of Frenkel Excitons in Molecular Aggregates. *Phys. Rep.* **2015**, *567*, 1–78.
- (21) Malý, P.; Somsen, O. J.; Novoderezhkin, V. I.; Mančal, T.; Van Grondelle, R. The Role of Resonant Vibrations in Electronic Energy Transfer. *ChemPhysChem* **2016**, *17*, 1356–1368.

- (22) Dean, J. C.; Mirkovic, T.; Toa, Z. S.; Oblinsky, D. G.; Scholes, G. D. Vibronic Enhancement of Algae Light Harvesting. *Chem* **2016**, *1*, 858–872.
- (23) Yeh, S.-H.; Hoehn, R. D.; Allodi, M. A.; Engel, G. S.; Kais, S. Elucidation of Near-Resonance Vibronic Coherence Lifetimes by Nonadiabatic Electronic-Vibrational State Character Mixing. *Proc. Natl. Acad. Sci. U.S.A.* **2019**, *116*, 18263–18268.
- (24) Arsenault, E. A.; Yoneda, Y.; Iwai, M.; Niyogi, K. K.; Fleming, G. R. Vibronic Mixing Enables Ultrafast Energy Flow in Light-Harvesting Complex II. *Nat. Commun.* **2020**, *11*, 1460.
- (25) Higgins, J. S.; Lloyd, L. T.; Sohail, S. H.; Allodi, M. A.; Otto, J. P.; Saer, R. G.; Wood, R. E.; Massey, S. C.; Ting, P.-C.; Blankenship, R. E. et al. Photosynthesis Tunes Quantum-Mechanical Mixing of Electronic and Vibrational States to Steer Exciton Energy Transfer. *Proc. Natl. Acad. Sci. U.S.A.* **2021**, *118*, e2018240118.
- (26) Policht, V. R.; Niedringhaus, A.; Willow, R.; Laible, P. D.; Bocian, D. F.; Kirmaier, C.; Holten, D.; Mančal, T.; Ogilvie, J. P. Hidden Vibronic and Excitonic Structure and Vibronic Coherence Transfer in the Bacterial Reaction Center. *Sci. Adv.* **2022**, *8*, eabk0953.
- (27) Wendling, M.; Pullerits, T.; Przyjalowski, M. A.; Vulto, S. I.; Aartsma, T. J.; van Grondelle, R.; van Amerongen, H. Electron-Vibrational Coupling in the Fenna-Matthews-Olson Complex of *Prosthecochloris a estuarii* Determined by Temperature-Dependent Absorption and Fluorescence Line-Narrowing Measurements. *J. Phys. Chem. B* **2000**, *104*, 5825–5831.
- (28) Rätsep, M.; Freiberg, A. Electron-Phonon and Vibronic Couplings in the FMO Bacteriochlorophyll a Antenna Complex Studied by Difference Fluorescence Line Narrowing. *J. Lumin.* **2007**, *127*, 251–259.

- (29) Klinger, A.; Lindorfer, D.; Müh, F.; Renger, T. Normal Mode Analysis of Spectral Density of FMO Trimers: Intra- and Intermonomer Energy Transfer. *J. Chem. Phys.* **2020**, *153*, 215103.
- (30) Duan, H.-G.; Nalbach, P.; Miller, R. D.; Thorwart, M. Intramolecular Vibrations Enhance the Quantum Efficiency of Excitonic Energy Transfer. *Photosynth. Res.* **2020**, *144*, 137–145.
- (31) Jiang, X.-P.; Brumer, P. Creation and Dynamics of Molecular States Prepared With Coherent vs Partially Coherent Pulsed Light. *J. Chem. Phys.* **1991**, *94*, 5833–5843.
- (32) Mančal, T.; Valkunas, L. Exciton Dynamics in Photosynthetic Complexes: Excitation by Coherent and Incoherent Light. *New J. Phys.* **2010**, *12*, 065044.
- (33) Brumer, P.; Shapiro, M. Molecular Response in One-Photon Absorption via Natural Thermal Light vs. Pulsed Laser Excitation. *Proc. Natl. Acad. Sci. U.S.A.* **2012**, *109*, 19575–19578.
- (34) Pachón, L. A.; Brumer, P. Computational Methodologies and Physical Insights Into Electronic Energy Transfer in Photosynthetic Light-Harvesting Complexes. *Phys. Chem. Chem. Phys.* **2012**, *14*, 10094–10108.
- (35) Kassal, I.; Yuen-Zhou, J.; Rahimi-Keshari, S. Does Coherence Enhance Transport in Photosynthesis? *J. Phys. Chem. Lett.* **2013**, *4*, 362–367.
- (36) Pachón, L. A.; Botero, J. D.; Brumer, P. W. Open System Perspective on Incoherent Excitation of Light Harvesting Systems. *J. Phys. B: At. Mol. Opt. Phys.* **2017**, *50*, 184003.
- (37) Brumer, P. Shedding (Incoherent) Light on Quantum Effects in Light-Induced Biological Processes. *J. Phys. Chem. Lett.* **2018**, *9*, 2946–2955.

- (38) Tomasi, S.; Kassal, I. Classification of Coherent Enhancements of Light-Harvesting Processes. *J. Phys. Chem. Lett.* **2020**, *11*, 2348–2355.
- (39) Calderón, L. F.; Pachón, L. A. Nonadiabatic Sunlight Harvesting. *Phys. Chem. Chem. Phys.* **2020**, *22*, 12678–12687.
- (40) Dodin, A.; Brumer, P. Noise-Induced Coherence in Molecular Processes. *J. Phys. B: At. Mol. Opt. Phys.* **2021**, *54*, 223001.
- (41) Calderón, L. F.; Chuang, C.; Brumer, P. Electronic-Vibrational Resonance Does Not Significantly Alter Steady-State Transport in Natural Light-Harvesting Systems. *J. Phys. Chem. Lett.* **2023**, *14*, 1436–1444.
- (42) Tscherbul, T. V.; Brumer, P. Non-Equilibrium Stationary Coherences in Photosynthetic Energy Transfer Under Weak-Field Incoherent Illumination. *J. Chem. Phys.* **2018**, *148*, 124114.
- (43) Chuang, C.; Brumer, P. LH1-RC Light-Harvesting Photocycle Under Realistic Light-Matter Conditions. *J. Chem. Phys.* **2020**, *152*, 154101.
- (44) Jung, K. A.; Brumer, P. Energy Transfer Under Natural Incoherent Light: Effects of Asymmetry on Efficiency. *J. Chem. Phys.* **2020**, *153*, 114102.
- (45) Pachón, L. A.; Brumer, P. Incoherent Excitation of Thermally Equilibrated Open Quantum Systems. *Phys. Rev. A* **2013**, *87*, 022106.
- (46) Tanimura, Y.; Kubo, R. Time Evolution of a Quantum System in Contact With a Nearly Gaussian-Markoffian Noise Bath. *J. Phys. Soc. Jpn.* **1989**, *58*, 101–114.
- (47) Tanimura, Y. Nonperturbative Expansion Method for a Quantum System Coupled to a Harmonic-Oscillator Bath. *Phys. Rev. A* **1990**, *41*, 6676–6687.

- (48) Ishizaki, A.; Tanimura, Y. Quantum Dynamics of System Strongly Coupled to Low-Temperature Colored Noise Bath: Reduced Hierarchy Equations Approach. *J. Phys. Soc. Jpn.* **2005**, *74*, 3131–3134.
- (49) Ishizaki, A.; Fleming, G. R. Unified Treatment of Quantum Coherent and Incoherent Hopping Dynamics in Electronic Energy Transfer: Reduced Hierarchy Equation Approach. *J. Chem. Phys.* **2009**, *130*, 234111.
- (50) Tanimura, Y. Numerically “Exact” Approach To Open Quantum Dynamics: The Hierarchical Equations of Motion (HEOM). *J. Chem. Phys.* **2020**, *153*, 020901.
- (51) Lambert, N.; Raheja, T.; Cross, S.; Menczel, P.; Ahmed, S.; Pitchford, A.; Burgarth, D.; Nori, F. QuTiP-BoFiN: A Bosonic and Fermionic Numerical Hierarchical-Equations-Of-Motion Library with Applications in Light-Harvesting, Quantum Control, and Single-Molecule Electronics. *Phys. Rev. Res.* **2023**, *5*, 013181.
- (52) Mandel, L.; Wolf, E. *Optical Coherence and Quantum Optics*; Cambridge University Press: Cambridge, 1995.
- (53) Janković, V.; Mančal, T. Nonequilibrium Steady-State Picture of Incoherent Light-Induced Excitation Harvesting. *J. Chem. Phys.* **2020**, *153*, 244110.
- (54) León-Montiel, R. d. J.; Kassal, I.; Torres, J. P. Importance of Excitation and Trapping Conditions in Photosynthetic Environment-Assisted Energy Transport. *J. Phys. Chem. B* **2014**, *118*, 10588–10594.
- (55) Nitzan, A. *Chemical Dynamics in Condensed Phases*; Oxford University Press: Oxford, 2006.
- (56) Roden, J. J.; Whaley, K. B. Probability-Current Analysis of Energy Transport in Open Quantum Systems. *Phys. Rev. E* **2016**, *93*, 012128.

- (57) Yang, P.-Y.; Cao, J. Steady-State Analysis of Light-Harvesting Energy Transfer Driven by Incoherent Light: From Dimers to Networks. *J. Phys. Chem. Lett.* **2020**, *11*, 7204–7211.